

Surface and grain-boundary energies in yttria-stabilized zirconia (YSZ-8 mol %)

A. TSOGA, P. NIKOLOPOULOS

Chemical Engineering Department and Institute of Chemical Engineering and High-Temperature Chemical Processes, University of Patras, GR 265 00 Patras, Greece

The multiphase equilibration technique has been used to measure the equilibrium angles that develop at the interphase boundaries of a solid–liquid–vapour system after annealing and also the surface (γ_{SV}) and the grain-boundary, (γ_{SS}) energies of polycrystalline yttria-stabilized zirconia (8 mol % Y_2O_3). The data was recorded in the temperature range 1573–1873 K. Linear temperature functions were obtained for the surface energy

$$\gamma_{SV} \text{ (J m}^{-2}\text{)} = 1.927 - 0.428 \times 10^{-3} T$$

and for the grain-boundary energy

$$\gamma_{SS} \text{ (J m}^{-2}\text{)} = 1.215 - 0.358 \times 10^{-3} T$$

1. Introduction

Yttria stabilized zirconia (YSZ) is the most commonly used material in solid oxide fuel cells (SOFC)'s technology finding application as an electrolyte and also as an anode material component. A significant area of current research in this field concerns the development of new composite materials with improved properties for application as cell components. A knowledge of the absolute values of surface and interfacial energies of the materials or the materials systems used is of great importance. This is because such information enables prediction of the properties of a new material, such as nucleation, sintering behaviour and mass transport phenomena. The aim of the present work is the direct determination of surface and grain-boundary energies of YSZ (8 mol % Y_2O_3) at elevated temperatures.

The multiphase equilibration technique is the most common experimental method [1, 2] used for the determination of surface and grain-boundary energies in polycrystalline materials at high temperatures. This technique involves the measurement of the equilibrium angles, shown in Fig. 1(a–c), that develop at interphase boundaries [3, 4] of a solid–liquid–vapour system after annealing. These angles are related to the surface and interfacial energies of the phases in contact by the equations:

$$\gamma_{SS} = 2\gamma_{SV}\cos(\psi/2) \quad (1)$$

$$\gamma_{SS} = 2\gamma_{SL}\cos(\phi/2) \quad (2)$$

$$\gamma_{SV} = \gamma_{SL} + \gamma_{LV}\cos(\theta) \quad (3)$$

where γ_{SV} and γ_{SS} are the surface and the grain-boundary energies of the solid respectively, γ_{SL} is the interfacial energy between solid and liquid and γ_{LV} the surface energy of the liquid. These equations are

schematically represented for Equation 1 by Fig. 1a, for Equation 2 by Fig. 1b and Equation 3 by Fig. 1c.

Equations (1–3) can be rearranged to yield:

$$\gamma_{SV} = \gamma_{LV}\cos\theta \frac{\cos(\phi/2)}{\cos(\phi/2) - \cos(\psi/2)} \quad (4)$$

and

$$\gamma_{SS} = 2\gamma_{LV}\cos\theta \frac{\cos(\phi/2)\cos(\psi/2)}{\cos(\phi/2) - \cos(\psi/2)} \quad (5)$$

The assumptions used in the formulation of Equations 4 and 5 are:

- (a) Equilibrium in the formation of the angles is attained.
- (b) The γ_{SS} terms in Equations 1 and 2 are interchangeable and therefore torque terms can be neglected [3].
- (c) The interfacial energies are independent of the orientation [4, 5].
- (d) The metal–vapour contaminations of the furnace atmosphere do not influence the surface energy of the solid and therefore can be neglected [6, 7].

The surface energy of the liquid metallic phase used in the determination of surface and grain-boundary energies of a polycrystalline solid, Equations 4 and 5, is available in the literature.

2. Experimental procedure

The round discs of 20 mm diameter and 130 μm thickness of polycrystalline yttria-stabilized-zirconia used in the experiments were prepared via tape casting using a commercially available 8 mol % Y_2O_3 -powder, (TZ-8Y, Tosoh) with a purity > 99.9%. The samples were sintered at 1600 °C for 1 h in air to a density > 95% theoretical density and a grain size of about

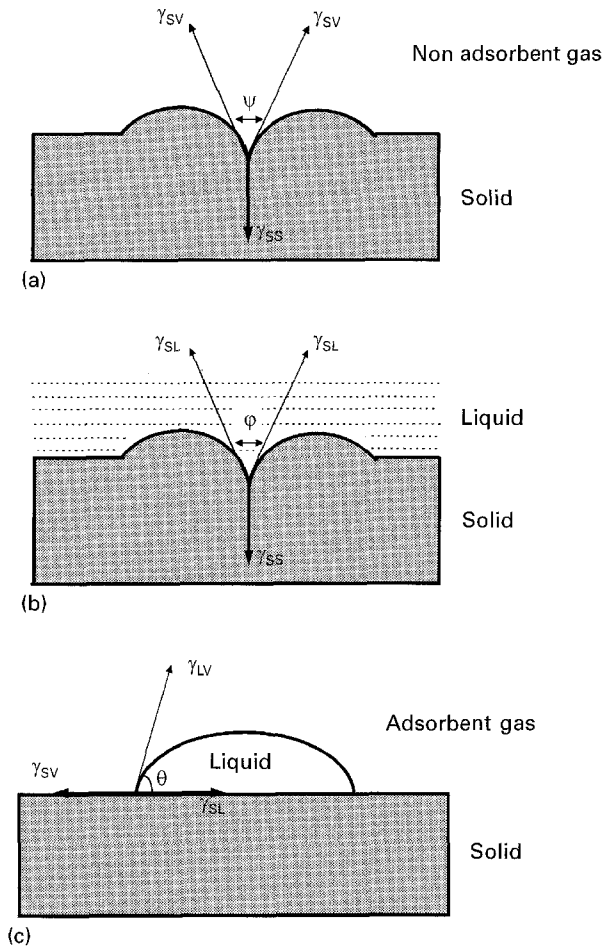


Figure 1 Schematic diagram illustrating interfacial equilibrium in (a) solid–solid–gas, (b) solid–solid–liquid and (c) solid–liquid–gas systems.

20 μm . All the samples were metallographically polished to a final roughness of 50 nm.

The metallic phases used were Sn and Ni with purities of 99.9985% and 99.9% respectively. These metallic elements were selected because they do not react with YSZ at the used experimental conditions.

The equilibration experiments concern the measurement of the groove angles ψ and ϕ and were performed in a SiC-resistance furnace. Sessile drop experiments, to measure the contact angle θ , were performed in an inductive furnace coupled with a molybdenum susceptor. In all cases the annealings occurred in a flowing purified Ar atmosphere.

Optical interferometry using a Leitz interferometer with a resolution limit of 0.3272 μm , was applied to the measurement of the groove angles, ψ and ϕ , the later being measured after the debonding of the metallic phase from the ceramic substrate.

The true root angles (ψ , ϕ) were calculated using; [8]

$$\tan(\psi, \phi/2) = \frac{2\delta}{1.11 \lambda m} \tan(\alpha/2) \quad (6)$$

where α and δ are the apparent root angle and the fringe spacing, respectively, measured from the interferometric patterns shown in Fig. 2. λ is the wavelength of the light source ($\lambda_{(\text{Na})} = 589 \text{ nm}$) and m the

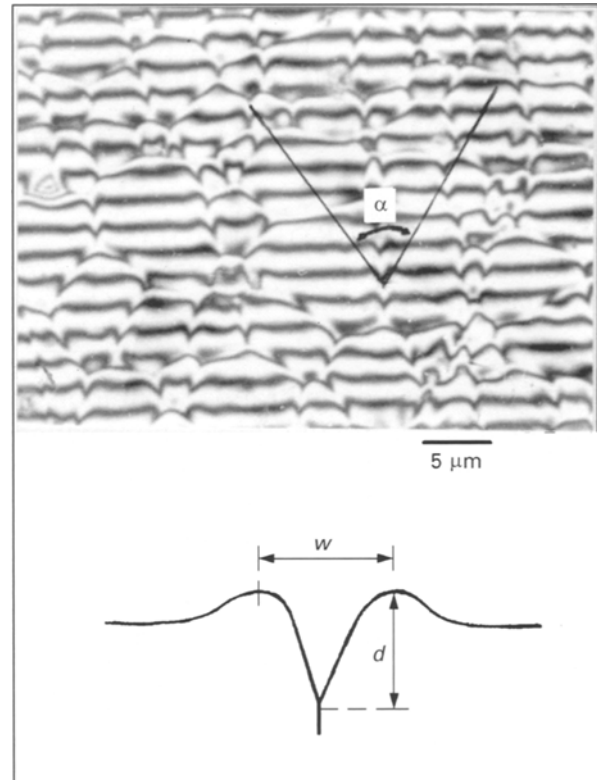


Figure 2 Interference pattern to obtain groove angle, ϕ , in the system YSZ/Sn ($T = 1573 \text{ K}$, $t = 21 \text{ h}$, $\lambda = 589 \text{ nm}$).

magnification. The factor 1.11 is a correction factor for the effect of the large aperture of the lens.

Contact angle, θ , measurements were able to be performed *in situ* since the inductive furnace, where the sessile drop experiments were performed, is coupled with a video-camera observation system.

The three sets of experiments were carried out at 1573, 1673, 1773 and 1873 K. The duration of the experiments had to be chosen so as to allow the grooves to obtain measurable dimensions of depth, d and width, w , of the groove shoulders, Fig. 2, (which of course had to be higher than the resolution limit of the interferometer) and also to allow the establishment of equilibrium. The durations used were 182 and 21 h at 1573 K, 65 and 3 h at 1673 K, 5, as well as 10 h and 70 min at 1773 K and 1 h and 30 min at 1873 K for the measurement of the angles ψ and ϕ , respectively.

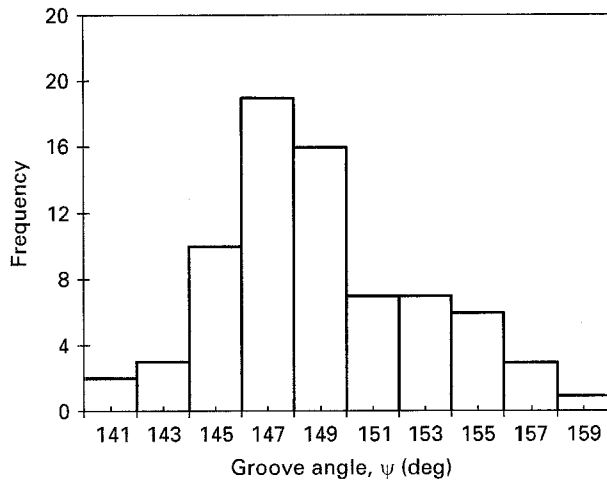
In the case of the sessile drop experiments an equilibrium contact angle, θ , was established during the first minutes of the experiments, that remained constant for the experimental time (20 min). Sn was used as the metallic phase for the temperatures 1573, 1673 and 1773 K. Ni was chosen for the temperature of 1873 K since at this temperature the vapour pressure of Sn becomes significant.

3. Results

Table I summarizes the calculated values of the groove angles, ψ and ϕ , with their mean standard errors. The reliability of the results depends on whether thermodynamic equilibrium is established under the experimental conditions. In this case equilibrium was

TABLE I Calculated values of groove angles ψ and ϕ with mean standard errors

T (K)	System	ψ (deg)	Number of measurements	System	ϕ (deg)	Number of measurements
1573	YSZ + Ar	149.0 ± 0.5	74	YSZ + Sn	155.1 ± 0.3	118
1673	YSZ + Ar	151.6 ± 0.3	36	YSZ + Sn	156.9 ± 0.2	127
1773	YSZ + Ar	151.8 ± 0.2	276	YSZ + Sn	155.8 ± 0.3	104
1873	YSZ + Ar	151.0 ± 0.4	51	YSZ + Ni	159.7 ± 0.2	88


 Figure 3 Typical distribution of groove angles, ψ , in YSZ/Ar at $T = 1573$ K for $t = 182$ h.

considered in terms of the development on the plane section of symmetrical grain-boundaries, forming angles of 120° between them at their intersections points. Since it is difficult to discriminate between grain-boundaries that are not perpendicular to the plane section, only those angles in which the interference pattern continued in approximately the same manner on both sides of the groove were considered, Fig. 2.

Another indication that equilibrium is approached is also the symmetrical distribution of the measured, angle values, as is shown in Fig. 3. Additionally, the fact that the pooled average of two such distributions for specimens annealed for 5 and 10 h at 1773 K was 151.8 with a standard deviation $\pm 3.3^\circ$ indicates that equilibrium is attained.

Table II includes the measured contact angle values, θ , as well as the surface energies of the liquid metals at the corresponding temperatures, as obtained from Equation 7 for Sn [9] and Equation 8 for Ni [10, 11]:

$$\gamma_{LV(\text{Sn})} = 0.544 - 0.07 \times 10^{-3}(T - 505) \quad (7)$$

and

$$\gamma_{LV(\text{Ni})} = 1.754 - 0.28 \times 10^{-3}(T - 1726) \quad (8)$$

In the case of sessile drop experiments the establishment of thermodynamic equilibrium was considered in terms of the maintenance of a constant value for the contact angle during the experiment.

From the experimental results listed in Tables I and II and using Equations 4 and 5 the values of the surface (γ_{SV}), and grain boundary (γ_{SS}), energies, as well as their ratio (γ_{SV}/γ_{SS}) were calculated. The results are included in Table III.

 TABLE II Measured contact angles values, θ , and surface energies of liquid metals

System	T (K)	θ (deg)	γ_{LV} (J m^{-2})
YSZ/Sn	1573	130.0	0.469
YSZ/Sn	1673	126.0	0.462
YSZ/Sn	1773	114.5	0.455
YSZ/Ni	1873	106.0	1.713

 TABLE III Calculated values of surface γ_{SV} , grain-boundary energy γ_{SS} and the ratio γ_{SS}/γ_{SV}

T (K)	γ_{SV} (J m^{-2})	γ_{SS} (J m^{-2})	γ_{SS}/γ_{SV}
1573	1.256 ± 0.129	0.674 ± 0.064	0.534 ± 0.008
1673	1.208 ± 0.142	0.592 ± 0.065	0.491 ± 0.005
1773	1.171 ± 0.176	0.571 ± 0.081	0.487 ± 0.003
1873	1.126 ± 0.097	0.563 ± 0.043	0.501 ± 0.007

The accuracy of the calculated values of the surface (γ_{SV}), and grain boundary, (γ_{SS}) energies is about $\pm 10\%$. It should be noted that the multiphase equilibration technique is sensitive to the values of the groove angles ψ and ϕ , whose measurement includes a statistical processing. Small deviations in the measurements could lead to significant deviations in the calculated energy values.

4. Discussion

Fig. 4 illustrates the temperature dependence of the calculated surface energy values, which can be described by the equation:

$$\gamma_{SV} = 1.927 - 0.428 \times 10^{-3}T, \quad R^2 = 0.99722 \quad (9)$$

The linear temperature coefficient (-0.428×10^{-3}) is in good agreement with corresponding values given in the literature for oxides with a cubic crystal structure such as calcia-stabilized zirconia, CSZ ($-0.431 \times 10^{-3} \text{ J} \cdot \text{m}^{-2} \cdot \text{K}^{-1}$) [7], UO_2 ($-0.351 \times 10^{-3} \text{ J} \cdot \text{m}^{-2} \cdot \text{K}^{-1}$) [2] and ThO_2 ($-0.24 \times 10^{-3} \text{ J} \cdot \text{m}^{-2} \cdot \text{K}^{-1}$) [12].

By extrapolation to a temperature of 3073 K which roughly corresponds to the melting point of YSZ, Equation 9 gives a surface energy value of $\gamma_{SV} = 0.578 \text{ J m}^{-2}$, which is comparable to that given by Lihrmann and Haggerty ($\gamma_{LV} = 0.43 \text{ J m}^{-2}$), [13], for pure liquid zirconia in air and it also yields similar behaviour to that observed in metals in that $\gamma_{SV}(T_{mp}) \approx 1.1\gamma_{LV}(T_{mp})$, [9].

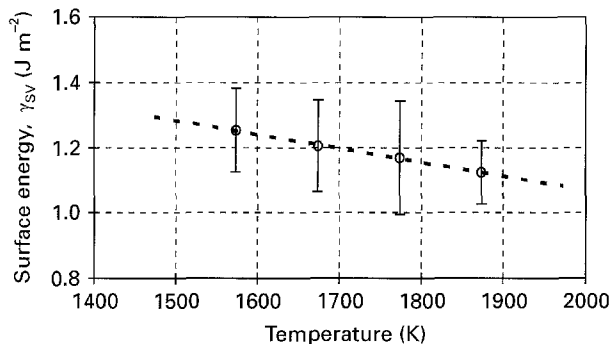


Figure 4 Temperature dependence of the surface energy of YSZ.

In the case of ZrO_2 stabilized with CaO the literature gives an equation for the calculation of the surface energy, of $\gamma_{sv} (\text{J m}^{-2}) = 1.428 - 0.431 \times 10^{-3} T$, [7], and also a value of 0.590 J m^{-2} at 2123 K , [14]. The equation produces lower energy values at the same temperature than those calculated for YSZ from Equation 9. A possible explanation for this discrepancy is the impurity content, of Al_2O_3 , SiO_2 and Fe_2O_3 , contained in the CSZ material. During annealing these impurities tend to concentrate on the surface and grain-boundaries of the material, resulting in a decrease of its surface energy, [14]. The value $\gamma_{sv} = 1.682 \text{ J m}^{-2}$ obtained by Equation 9 at 573 K is also higher compared to the value $\gamma_{sv} = 1.1 \text{ J m}^{-2}$ given for t-ZrO_2 , [15], measured using the heat of immersion technique.

Fig. 5 shows the calculated values of the grain-boundary energy of YSZ as a function of temperature. Considering a linear dependence between the grain-boundary energy and the temperature this relationship could be expressed as:

$$\gamma_{ss}(\text{J m}^{-2}) = 1.215 - 0.358 \times 10^{-3} T, \quad R^2 = 0.8094 \quad (10)$$

The linear temperature coefficient of γ_{ss} , ($-0.358 \times 10^{-3} \text{ J} \cdot \text{m}^{-2} \cdot \text{K}^{-1}$) closely agrees with the corresponding value ($-0.392 \times 10^{-3} \pm 0.126 \text{ J} \cdot \text{m}^{-2} \cdot \text{K}^{-1}$) calculated for CSZ in the temperature range $1173 \text{ K} \leq T \leq 1523 \text{ K}$, [7]. By extrapolation (Equation 10) at a temperature of 1523 K the value obtained ($\gamma_{ss} = 0.670 \text{ J m}^{-2}$) is in accordance with the value given by Chaim *et al.* [16] of 0.81 J m^{-2} , which was calculated using the model formulated by Read and Shockley [17] for a low-angle subboundary of edge dislocations, which would be applicable to the cubic/tetragonal semicoherent interfaces in two-phase ZrO_2 -8 wt % Y_2O_3 .

Literature values of γ_{ss} reported for CSZ are 0.489 – 0.348 J m^{-2} for temperatures between 1173 – 1523 K , [7], 0.265 J m^{-2} at 2123 K , [14] and 0.38 J m^{-2} at 1500 K [18] and are lower than the values calculated by the extrapolation of Equation 10 at the same temperatures. The differences between the above values, even if not significant, could be explained by the different composition of the corresponding materials.

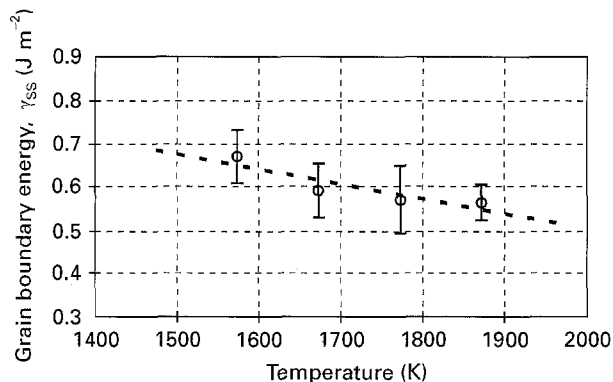


Figure 5 Temperature dependence of the grain-boundary energy of YSZ.

According to the results of Table III the ratio γ_{ss}/γ_{sv} , does not vary significantly with temperature and ranges between 0.487 – 0.534 . The constancy of the ratio γ_{ss}/γ_{sv} results from the fact that the groove angle value (ψ) remains practically constant with temperature, a phenomenon also observed in Al_2O_3 [19] and CSZ [7]. This phenomenon could be explained by the parallel increase of the groove width, w , and depth, d , Fig. 2, as a function of the temperature. The value of the ratio γ_{ss}/γ_{sv} calculated for YSZ is comparable with corresponding values for other oxides such as CSZ (0.45 – 0.53) [7], and (0.45) [14], and UO_2 (0.54 – 0.67) [1] and (0.54 – 0.58) [2], which as has already been mentioned have a cubic fluoride structure as does YSZ.

5. Summary

Using the multiphase equilibration technique the surface and grain-boundary energies of YSZ were determined in the temperature range $1573 \text{ K} \leq T \leq 1873 \text{ K}$, from measurement of the equilibrium groove angles, ψ , ϕ , and contact angles, θ . Both energy values were found to be linear functions of temperatures, which could be described by the equations:

$$\gamma_{sv}(\text{J m}^{-2}) = 1.927 - 0.428 \times 10^{-3} T$$

and

$$\gamma_{ss}(\text{J m}^{-2}) = 1.215 - 0.358 \times 10^{-3} T$$

The ratio γ_{ss}/γ_{sv} ranges between 0.487 – 0.534 and is in accordance with values measured for other oxides having a similar crystal structure.

Acknowledgement

This work was supported by E.C. JOU2-CT92-0063 research project.

References

1. E. N. HODKIN and M. G. NICHOLAS, *J. Nucl. Mater.* **47** (1973) 23.
2. P. NIKOLOPOULOS, S. NAZARE and F. THUEMLER, *ibid.* **71** (1977) 89.
3. B. K. HODGSON and H. MYKURA, *J. Mater. Sci.* **8** (1973) 565.

4. S. K. RHEE, *J. Amer. Ceram. Soc.* **55** (1972) 300.
5. W. M. ROBERTSON and P. CHANG, in "Materials Science Research", Vol. 3, edited by W. W. Kriegel and H. Palmour III, (Plenum Press, New York, 1966) p. 49.
6. P. NIKOLOPOULOS, *J. Mater. Sci.* **20** (1985) 3993.
7. D. SOTIROPOULOU and P. NIKOLOPOULOS, *ibid.* **26** (1991) 1395.
8. S. AMENLICKX, N. F. BINNENDIJK and W. DEKEYSER, *Physica* **19** (1953) 1173.
9. B. C. ALLEN, in "Liquid Metals", edited by S. Z. Beer (M. Dekker, New York, 1972) p. 161.
10. G. LANG, *Z. Metallkde* **68** (1977) 213.
11. A. R. MIEDEMA and R. BOOM, *Z. Metallkde* **69** (1978) H.3.
12. T. INOUE and H. J. MATZKE, *J. Amer. Ceram. Soc.* **64** (1981) 355.
13. J. M. LIHRMANN and J. S. HAGGERTY, *ibid.* **68** (1985) 81.
14. W. D. KINGERY, *ibid.* **37** (1954) 42.
15. H. F. HOLMES, E. L. FULLER and R. B. GAMMAGE, *J. Phys. Chem.* **76** (1972) 1497.
16. R. CHAIM, A. H. HEUER and D. G. BRANDON, *J. Amer. Ceram. Soc.* **69** (1986) 243.
17. W. T. READ and W. SHOCKLEY, *Phys. Rev.* **78** (1950) 275.
18. P. NIKOLOPOULOS, G. ONDRACEK and D. SOTIROPOULOU, *Ceram. Int.* **15** (1989) 201.
19. A. TSOGA and P. NIKOLOPOULOS, *J. Amer. Ceram. Soc.* **77** (1994) 954.

*Received 14 August 1995
and accepted 13 February 1996*